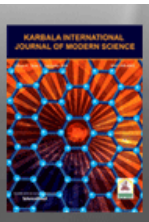
Karbala International Journal of Modern Science

Manuscript 3426

Impact of Plasma-Activated Water on Breast Cancer Cell Viability

Maryam G. Jasim

Hammad R. Humud

Follow this and additional works at: https://kijoms.uokerbala.edu.iq/home

Part of the Biology Commons, Chemistry Commons, and the Physics Commons

University of Kerbala

Impact of Plasma-Activated Water on Breast Cancer Cell Viability

Abstract

Plasma-activated water (PAW) was generated using a dielectric barrier discharge (DBD) plasma system operating with a 1:1 mixture of nitrogen and argon gases to evaluate its cytotoxic effects on MCF-7 breast cancer cells. Water samples were divided into five groups: 0 minutes (control), 5, 10, 15, and 20 minutes of plasma exposure. The resulting PAW was applied to cultured cells, and cell viability was assessed 24- and 48-hour post-treatment. Viability was evaluated using the 3-(4,5-dimethylthiazol-2-yl)-2,5-diphenyltetrazolium bromide (MTT) assay. The results showed an apparent time-dependent increase in cytotoxicity. At 24 hours, cell mortality rates were 1.9%, 40.7%, 48.1%, 53.6%, and 65.4%, while at 48 hours, they increased to 1.9%, 50.7%, 55.6%, 65.1%, and 74.93%. In addition, apoptosis-related analyses, mitochondrial membrane potential (MMP), viable cell count (VCC), and Total Nuclear Integrity (TNI), were used to study the induction of programmed cell death after PAW exposure. Comparative analysis with normal breast epithelial cells detected a significantly low cytotoxic reaction, indicating the selective anticancer potential of PAW. These findings highlight the PAW as a promising, selective, and non-thermal therapeutic agent for breast cancer treatment

Keywords

MCF-7 breast cancer cells; Plasma-activated water (PAW); Dielectric barrier discharge (DBD) plasma; Argon and nitrogen plasma; Reactive Oxygen and Nitrogen Species (RONS); MTT assay

Creative Commons License

This work is licensed under a Creative Commons Attribution-Noncommercial-No Derivative Works 4.0 License.

RESEARCH PAPER

Impact of Plasma-activated Water on Breast Cancer Cell Viability

Maryam G. Jasim*, Hammad R. Humud

Department of Physics, College of Science, University of Baghdad, Baghdad, Iraq

Abstract

Plasma-activated water (PAW) was generated using a dielectric barrier discharge (DBD) plasma system operating with a 1:1 mixture of nitrogen and argon gases to evaluate its cytotoxic effects on MCF-7 breast cancer cells. Water samples were divided into five groups: 0 min (control), 5, 10, 15, and 20 min of plasma exposure. The resulting PAW was applied to cultured cells, and cell viability was assessed 24- and 48-h post-treatment. Viability was evaluated using the 3-(4,5-dimethylthiazol-2-yl)-2,5-diphenyltetrazolium bromide (MTT) assay. The results showed an apparent time-dependent increase in cytotoxicity. At 24 h, cell mortality rates were 1.9 %, 40.7 %, 48.1 %, 53.6 %, and 65.4 %, while at 48 h, they increased to 1.9 %, 50.7 %, 55.6 %, 65.1 %, and 74.93 %. In addition, apoptosis-related analyses, mitochondrial membrane potential (MMP), viable cell count (VCC), and Total Nuclear Integrity (TNI), were used to study the induction of programmed cell death after PAW exposure. Comparative analysis with normal breast epithelial cells detected a significantly low cytotoxic reaction, indicating the selective anticancer potential of PAW. These findings highlight the PAW as a promising, selective, and non-thermal therapeutic agent for breast cancer treatment.

Keywords: MCF-7 breast cancer cells, Plasma-activated water (PAW), Dielectric barrier discharge (DBD) plasma, Argon and nitrogen plasma, Reactive oxygen and nitrogen species (RONS), MTT assay

1. Introduction

The ionized plasma medium comprises electrically charged particles and electrically neutral ones [1]. Plasma exhibits special physical features and chemical characteristics, enabling its use in multiple and advanced scientific applications [2]. Cold atmospheric pressure plasma (CAP) has shown substantial promise in biomedicine — notably for disinfection (including instrument sterilization), accelerating wound healing, and providing anticancer effects [3]. Plasma-activated water (PAW) has recently emerged as a promising plasma-based technique in medicine [4]. It is generated through plasma−liquid interactions that enrich the water with reactive oxygen and nitrogen species (RONS), which have demonstrated anticancer potential in recent studies [5]. DBD plasma stands out among different plasma sources for generating PAW because it creates highly reactive environments without needing extreme heat levels to protect treated solutions from medium instability [6]. The use of argon and nitrogen gases in dielectric barrier discharges has been shown to individually support the generation of various reactive species, including OH, NO, and H_2O_2, with argon enhancing discharge intensity and nitrogen enabling RNS formation [7], which amplifies the anti-cancer properties of PAW [8]. In dielectric barrier discharge (DBD)-based plasma, the use of gases such as argon and nitrogen facilitates the generation of long-lived reactive oxygen and nitrogen species (RONS), including NO and NO_2^-, which are critical for modulating the tumor microenvironment [9]. Produced RONS from PAW interactions can connect with vital cell components, which creates oxidative stress that modifies mitochondrial function while triggering apoptotic

Received 29 April 2025; revised 20 July 2025; accepted 2 August 2025.
Available online 15 September 2025

* Corresponding author.
E-mail addresses: mariam.jassem2404p@sc.uobaghdad.edu.iq (M.G. Jasim), Hamid.r@sc.uobaghdad.edu.iq (H.R. Humud).

https://doi.org/10.33640/2405-609X.3426
2405-609X/© 2025 University of Kerbala. This is an open access article under the CC-BY-NC-ND license (http://creativecommons.org/licenses/by-nc-nd/4.0/).

pathways [10]. The efficiency of PAW production depends on the composition of working gas and applied energy, as both influence the generation of reactive plasma species. Specifically, the O_2/N_2 ratio under atmospheric-pressure conditions shapes the ROS/RNS balance, while energy input governs their abundance and activity. These parameters significantly affect plasma chemistry and species evolution [11,12].

Studies show that plasma-activated medium (PAM) and plasma-activated water (PAW) reduce breast cancer cell viability. PAM alters membrane integrity and promotes ROS-mediated cell death [13], while PAW independently affects membrane properties and induces oxidative stress in cancer cells [14]. The MTT assay is a standard technological method that evaluates cytotoxicity and measures the effectiveness of anticancer therapy. This assay determines cell metabolic activity through the cellular conversion of MTT dye to produce formazan, which can be quantified spectrophotometrically [15]. Plasma-activated water (PAW) significantly reduces the viability of breast cancer cells, such as MCF-7, by inducing oxidative stress. This effect arises from the reactive species generated during plasma activation, which disrupt cellular metabolism and inhibit proliferation pathways [16]. Moreover, the combined use of argon with nitrogen in PAW production methods proves more effective than using either gas independently. This mixture creates an ideal balance of reactive molecules that improves cancer cell destruction [17]. The research investigates breast cancer cell susceptibility to plasma-treated water with an argon/nitrogen gas mixture through an MTT assay following periods of 24 and 48 h. This study compares the effects of argon and nitrogen gas combination on breast cancer cells against previous studies using alternative gas treatments or plasma concentrations to validate PAW as an alternate breast cancer therapy. Unlike many previous studies, which depended on individual gas plasma systems such as Argon or Helium, this research employs a dielectric barrier discharge (DBD) system using a binary mix of argon and nitrogen to increase the production of reactive nitrogen species (RNS) in plasma-active water (PAW). By systematically examining the physical and chemical properties of PAW-PH, ORP, and H_2O_2, NO_2^-, and NO_3^- concentrations, with timely cytotoxic effects on breast cancer cells, this study offers a novel insight into the gas-refined PAW system in plasma oncology. The purpose is to generate basic data that supports cold plasma, based on physical and chemical interactions, as a promising cancer treatment method.

1.1. Mechanism of RONS generation in PAW

The discharge of plasma over water through a mixture of argon and nitrogen gases initiates physical and chemical processes that yield RONS. Argon plays a key role by creating free electrons from its low ionization energy to activate both nitrogen molecules and water dissociation and excitation. Energetic electrons create RONS by disrupting gaseous and water molecules and prompting secondary chemical processes within the water solution [18]. Key reactions include:

$$e^- + Ar \rightarrow Ar^* + e^-$$

$$Ar^* + N_2 \rightarrow N_2^* + Ar$$

$$e^- + H_2O \rightarrow H\cdot + OH\cdot + e^-$$

$$N_2 + e^- \rightarrow 2N + e^-$$

$$N + O_2 \rightarrow NO + O$$

$$NO + OH\cdot \rightarrow NO_2^- + H^+$$

$$OH\cdot + OH\cdot \rightarrow H_2O_2$$

During these reactions, hydrogen peroxide (H_2O_2), nitrite (NO_2^-), and nitrate (NO_3^-) are formed as species that significantly affect PAW's biological activity [19,20].

2. Materials and methods

2.1. Setup of the DBD plasma

The experimental DBD plasma reactor appears in Fig. 1 through its schematic diagram. The plasma system contains a cylindrical Teflon cavity functionally designed as the discharge chamber. The cavity includes a tumbler tube as its main component, with a 10 cm length and 2 mm thickness. The tube features an open design that allows contact with plasma environmental conditions at its bottom end. The Teflon cavity contains a 16 mm diameter copper electrode with a 15.5 cm length. A disc-shaped termination exists at the end of this electrode with dimensions of 3 mm in thickness and 2 mm in width inside the glass tube. The adjustable position of the copper electrode enables users to control the plasma conditions perfectly. The copper electrode has a disc-shaped end, and a

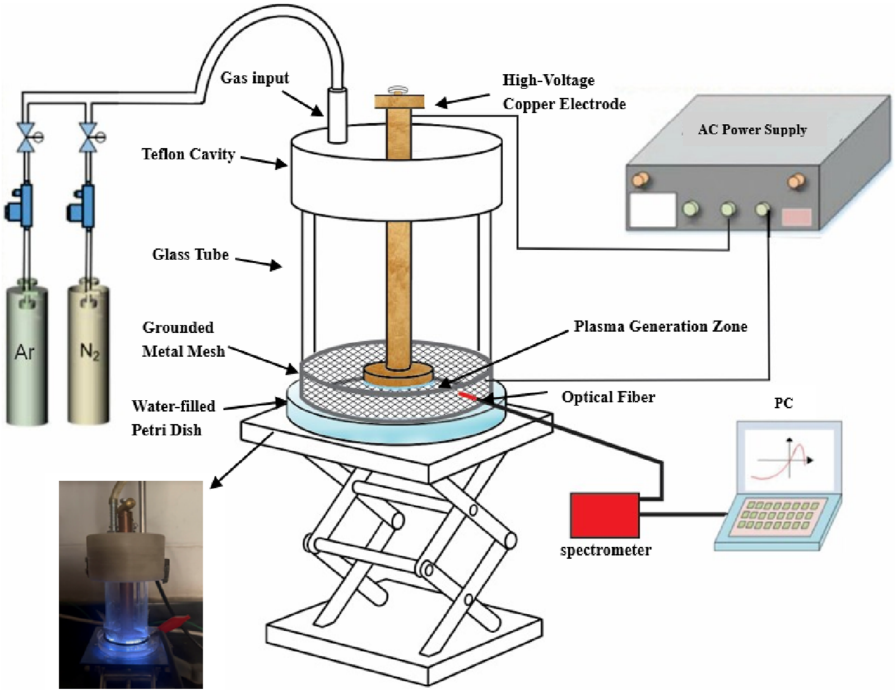

Fig. 1. Schematic diagram of the DBD plasma reactor.

1.5 mm-thick 40 mm diameter quartz plate is an insulating protection surface. The lower part of the glass tube contains a metal mesh securing the second electrode. Such a design and a metal mesh allow for the consistent operation of stable DBD plasma technology. Through the upper Teflon cavity inlet, gas enters the device using a 5 mm diameter and 8 mm connector to maintain precise gas delivery at the release site. A mechanical adjustable stage supports the setup to maintain accurate device positioning control. The presented schematic provides a visual representation of the machine configuration setup. The system functions through alternating current (AC) energy at a 20 kHz frequency, which generates an output voltage of 20 kV. The supplied power enables the device to create suitable electrical discharges. The frequency adjustment occurs within this range to control plasma properties and achieve optimal target medium engagement. The power supply makes a DBD or plasma jet device through controlled operation parameters. High-voltage breakers, appropriate electrical insulators, and a robust grounding system, combined with safety elements, can protect the device by ensuring efficient operation.

2.2. Sample preparation

A 0.9 % sodium chloride (NS) medical solution served as the water supply in 15 ml. The medical solution originated from Gulf Inject LLC in Dubai, UAE, where each 100 ml vial contained 0.9 g NaCl substance at a concentration level of 0.9 % and an osmotic concentration of 308 mOsm/L. It was used without purification or modification. The solution was activated using the plasma system designed for this study, exposing the sample to 5, 10, 15, or 20 min with DBD plasma using argon and nitrogen at a flow rate of 2.5 L/min for each gas.

2.3. Physicochemical analysis of PAW

The concentrations of RONS in PAW were quantified utilizing commercial test strips from Bartovation (USA), following the manufacturer's guidelines. The analysis encompassed the concentrations of hydrogen peroxide (H_2O_2), nitrate (NO_3^-), and nitrite (NO_2^-) in plasma-treated samples. Hydrogen peroxide (H_2O_2) was detected with Bartovation Peroxide Test Strips (PPX03V100, USA), which have a detection range of 0–400 ppm. The test strip was dipped into the sample for 1 s, excess liquid was removed, and after 10–30 s, the color was compared to the reference chart to determine the concentration. Nitrate (NO_3^-) and nitrite (NO_2^-) concentrations were measured using test strips with a 0–500 ppm detection range, following the same dip, wait, and evaluation technique. All measurements were conducted under controlled conditions, and results were recorded at

different plasma exposure times (0, 5, 10, 15, and 20 min). The obtained values were analyzed to observe changes in RONS concentrations over time. The activated water's electrical conductivity and oxidation-reduction potential (ORP) were measured using a multi-parameter device with appropriate probes, following standard procedures for assessing the physicochemical properties of liquids. Semi-quantitative strips were used; spectrophotometric validation is recommended for future studies.

2.4. Optical emission spectroscopy (OES)

Plasma emission spectra were obtained using a compact CCD spectrometer (Model CCS100/M, Thorlabs GmbH, Germany), operating across the 320–740 nm wavelength range with a spectral resolution of less than 0.5 nm at 435 nm. The spectrometer was connected to a quartz optical fiber with a focusing lens, positioned perpendicular to the plasma discharge at a constant distance of approximately 2 cm. Data acquisition and peak analysis were conducted with Thor Spectra software (version 3.35.0.3768, Thorlabs, Sweden). Emission lines for significant reactive species, including OH (309 nm), N_2 (337 nm), and O (777 nm), were detected to confirm the production of RONS by the plasma.

2.5. Cell culture

MCF-7 breast cancer cells were cultured according to established protocols for cell lines [21]. The cells were cultured in two media types: RPMI-1640 supplemented with L-glutamine, 10 % fetal bovine serum (FBS), and 1 % penicillin-streptomycin. Incubation was carried out in a humidified environment with 5 % CO_2 at 37 °C. Upon reaching confluency, the cells were passaged using trypsin-EDTA. Also, one line of a normal human breast epithelial cell line (MCF-10A) was cultured in Dulbecco's Modified Eagle Medium (DMEM) supplemented with 10 % fetal bovine serum (FBS) and 1 % penicillin–streptomycin [22]. PAW was added to the cells seeded in 96-well plates, and the cells were treated for 24 and 48 h.

2.6. MTT assay

MCF-7 breast cancer cells (1×10^4 cells/well) were seeded into 96-well plates containing complete DMEM supplemented with L-glutamine. Once the cells reached the precise confluency, the culture medium was removed, and the cells were immediately exposed to high concentrations of activated water for 2 h without any culture medium. The researchers discarded activated water from the wells before replacing them with a new DMEM medium. Two different incubation durations of 24 and 48 h were used for the cells under 37 °C conditions at 5 % CO_2 humidity. Each well received a fresh DMEM measurement of 100 μL before adding 10 μL containing a 12 mM MTT stock solution at the end of the incubation time points. Under identical conditions, the plates were further incubated for 3–4 h. Each well received 100 μL of dimethyl sulfoxide (DMSO) for dissolving the formazan crystals after solution removal [13]. Absorbance was quantified at 570 nm using an ELISA reader (Benchmark Microplate Reader, Bio-Rad). Cell viability was determined using the following formula:

$$(A_{\text{-treated}} - A_{\text{-blank}}) / (A_{\text{-control}} - A_{\text{-blank}}) \times 100$$

Where:

$A_{\text{-treated}}$ represents the absorbance measured in wells containing activated water.

$A_{\text{-control}}$ refers to the absorbance in untreated control wells.

$A_{\text{-blank}}$ represents the absorbance in cell-free wells.

All experiments were conducted in triplicate to ensure statistical reliability [23]. The same MTT assay protocol was applied to both MCF-7 and MCF-10A cell lines.

2.7. Apoptosis evaluation

MCF-7 breast cancer cells were incubated for 24 h. A multi-parameter fluorescence-based apoptosis detection kit (manufacturer BioLegend) performed apoptosis quantification. Viable Cell Count (VCC), Total Nuclear Integrity (TNI), and Mitochondrial Membrane Potential (MMP) were key indicators that were analyzed. Each condition was performed in triplicate, and fluorescence intensity readings were obtained with a microplate reader. Statistical significance was measured using one-way ANOVA, followed by data analysis using GraphPad Prism software (version 9.5.1) and Dunnett's multiple comparisons test. Statistically significant was considered at $p < 0.05$.

3. Results and discussion

3.1. Optical emission spectra

Optical emission spectroscopy (OES) was used to analyze the plasma generated by a DBD system when combining nitrogen (N_2) and argon (Ar)

gases. The spectrum showed several distinct spectral peaks, reflecting the presence of excited species in the plasma environment, as illustrated in Fig. 2. For nitrogen plasma, distinct emissions were observed due to excited nitrogen molecules, with prominent spectral peaks appearing at 337.48 nm (N_2 SPS 0→0), 357.69 nm (N_2 SPS 0→1), 378.93 nm (N_2 SPS 0→2), and 390.474 nm (N_2 SPS 1→3). These emissions correspond to vibrational transitions in the Second Positive System ($C^3\Pi_u \rightarrow B^3\Pi g$) of N_2, resulting from electron impact excitation in the plasma. Additionally, a strong peak at 308.9 nm was attributed to the OH ($A^2\Sigma^+ \rightarrow X^2\Pi$) transition, indicating the presence of hydroxyl radicals generated from water vapor dissociation. For argon plasma, emission lines were detected from excited argon atoms (Ar I) and argon ions (Ar II). Peaks attributed to Ar I were observed at 588.454, 602.515, 617.017, 635.702, 660.401,696.543,705.499,714.704, 750.515, 762.888, and 772.420 nm. In comparison, peaks at 680.853 nm and 738.042 nm were identified as originating from Ar II, as verified using the NIST Atomic Spectra Database. This indicates the ionization of some argon atoms due to the high energy of the electrons, contributing to a plasma environment rich in energetic particles and active chemical species. These results confirm that the produced plasma contains an environment rich in excited species, ions, and active chemical radicals, making it directly influential in the reactions of PAW and its various applications in medical and environmental fields [24]. Every spectral line from plasma elements was the basis for calculating electron temperature through the Boltzmann method [25]. The experimental findings confirmed an electron temperature of 1.1 eV, while the measurement outcomes depended on both applied voltage strength and gas mixture composition [26]. These outcomes matched earlier investigations [27].

3.2. Physicochemical parameters

Plasma exposure in Fig. 3 and Table 1 resulted in a mild rise in water temperature from 10.9 °C to 16.0 °C during 20 min. The temperature increase of 5.1 °C was not extensive, but it might have improved the diffusion patterns of reactive molecules and their overall activity. The primary cause of temperature increase involves energetic electron collisions between the plasma-liquid boundary and the production of heated aqueous phase regions. The development process leads to stepwise ion accumulation of H^+, NO_3^-, and NO_2^-. The solution's conductivity increases because plasma activates chemical reactions that produce reactive nitrogen species, including nitric acid (HNO_3) and

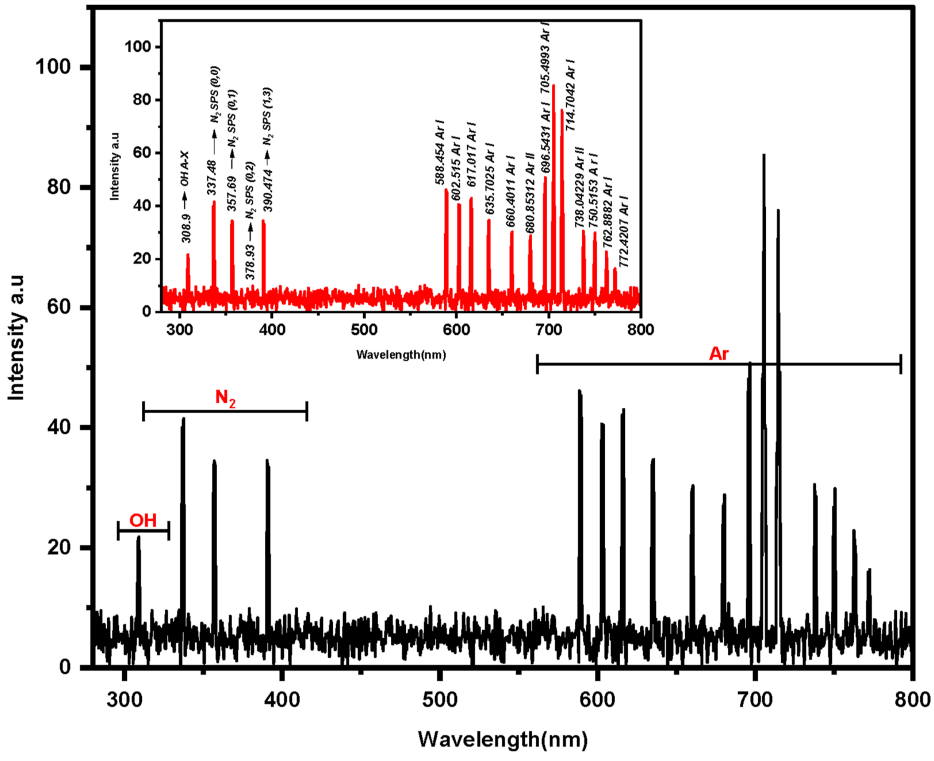

Fig. 2. Spectrum of DBD plasma with N_2 and Ar gases.

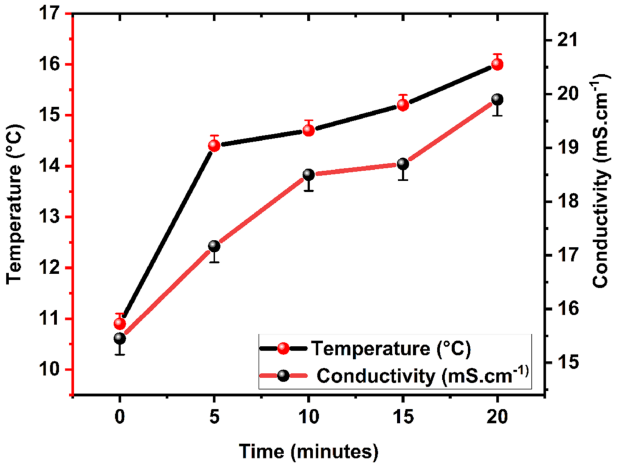

Fig. 3. Changes in temperature and electrical conductivity of PAW over time.

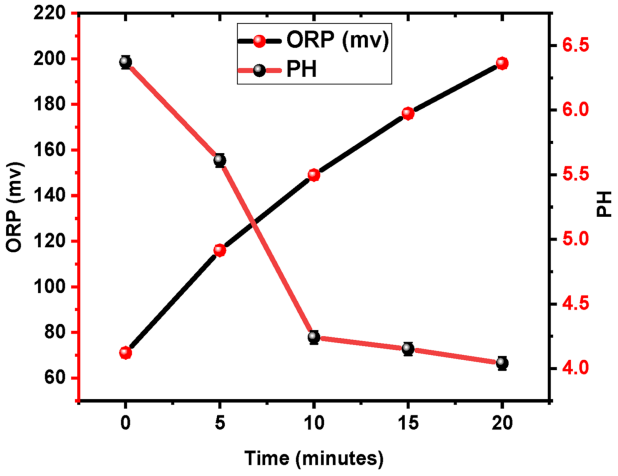

Fig. 4. Changes in PH and ORP of PAW over time.

nitrous acid (HNO_2), which dissociate into ions. The test results showed elevated electrical conductivity values from 15.54 to 19.9 mS/cm due to plasma treatment, extending the duration of exposure. This result confirmed reactive ionic species build-up over time. Various physicochemical properties that scientists measured indicate that plasma-liquid interactions lead to ionization processes and energy transfer effects, which transform water into an activated medium that can be used for multiple applications [28].

3.3. Acidification and redox dynamics

An apparent pH decrease from 6.37 to 4.07 showed acidification occurred because of weak acid generation, including nitric acid (HNO_3) and nitrous acid (HNO_2). Acidification results from nitrogen oxide (NO, NO_2, N_2O_5) solubility in the plasma discharge that produces combined reactions with water molecules to create HNO_2 and HNO_3 acid species. These acids give off H^+ ions upon dissociation, lowering the pH reading. The experiments showed how the oxidation-reduction potential (ORP) measurement elevated from 71 mV to 198 mV, demonstrating a clear transformation toward increased oxidation, as shown in Fig. 4 and Table 2. This increase reflects the accumulation of potent oxidizing agents such as hydrogen peroxide

Table 1. PAW temperature and conductivity over time.

Time (minutes)	Temperature (°C)	Conductivity (mS·cm^{-1})
0	10.9	15.45
5	14.4	17.17
10	14.7	18.5
15	15.2	18.7
20	16	19.9

Table 2. ORP and pH values of plasma-activated water.

Time (minutes)	ORP (mv)	PH
0	71	6.37
5	116	5.61
10	149	4.24
15	176	4.15
20	198	4.04

(H_2O_2), reactive nitrogen species (RNS) like NO_2^- and peroxynitrite, generated during plasma-liquid interactions. The high ORP indicates a strong capacity to accept electrons, enhancing the antimicrobial and oxidative reactivity of the water [29].

3.4. Reactive chemical inventory (RONS)

During plasma activation of water, our experimental results Fig. 5 showed a progressive increase

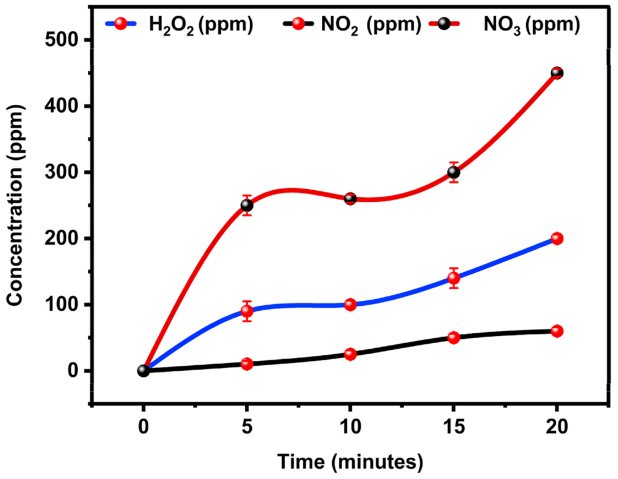

Fig. 5. Time-dependent conversion of nitrite (NO_2^-), nitrate (NO_3^-), and (H_2O_2) in PAW.

in the concentrations of hydrogen peroxide (H_2O_2) and nitrate (NO_3^-) over time, due to ongoing plasma–liquid chemical interactions. H_2O_2 forms primarily through the recombination of hydroxyl radicals (•OH), which are generated when energetic electrons or UV photons dissociate water molecules. NO_3^-, on the other hand, is produced through the dissolution of nitrogen oxides (NO, NO_2, N_2O_5) from the plasma gas phase into water, followed by redox reactions, particularly in the presence of potent oxidizing agents such as H_2O_2 and ozone (O_3). The accumulation of reactive species in PAW reflects its oxidative richness and supports its use in disinfection, cancer therapy, and seed germination [30–32].

In our results, nitrite (NO_2^-) and nitrate (NO_3^-) are both products of plasma-derived nitrogen chemistry—initially, NO_2^- forms from the dissolution of nitrogen dioxide (NO_2) into the aqueous phase. As observed in our study, NO_2^- is gradually oxidized to NO_3^- with increased exposure time in the presence of strong oxidants such as hydrogen peroxide (H_2O_2) and ozone (O_3), as shown in Fig. 5. This sequential conversion recorded in our experimental system reflects a time-dependent redox cascade, where NO_2^- serves as an intermediate. This behavior is critical in biomedical applications due to the roles of NO_2^- and NO_3^- in cellular signaling and antimicrobial action [33].

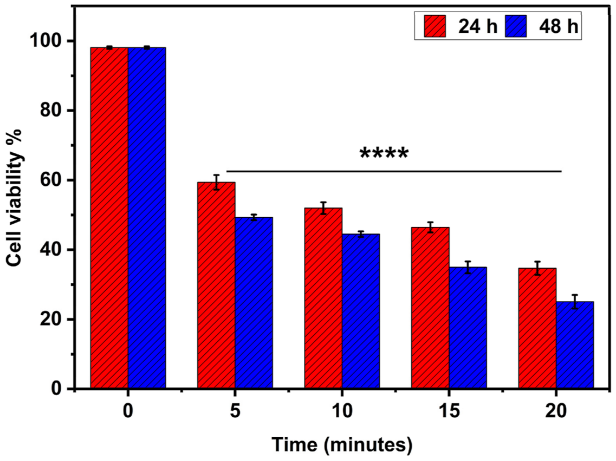

Fig. 6. MTT assay results for MCF-7 breast cancer cells treated with PAW.

3.5. MTT assay

The MTT assay is a well-established method for evaluating treatments' cytotoxic potential by measuring viable cells' metabolic activity [22]. In this study, Water was exposed to plasma for 0, 5, 10, 15, and 20 min, then applied to MCF-7 breast cancer cells. Cell viability was assessed after 24 and 48 h of incubation to examine both the duration of plasma exposure and the extended cellular response. The results revealed an apparent time-dependent cytotoxic effect of PAW. As shown in Fig. 6 and Table 3, increasing plasma exposure time significantly decreased cell viability, indicating enhanced toxicity with longer activation times. At 24 h, cell viability dropped from 98.11 % ± 0.35 in the control group to 34.68 % ± 1.91 for PAW generated after 20 min of plasma exposure. After 48 h, the cytotoxic effect became more pronounced, with viability decreasing further to 25.08 % ± 1.96, suggesting cumulative oxidative damage over time. This trend is attributed to the increasing accumulation of RONS in the PAW, such as hydrogen peroxide (H_2O_2), nitrite (NO_2^-), nitrate (NO_3^-), and peroxynitrite ($ONOO^-$). These species induce oxidative stress within cancer cells, leading to mitochondrial dysfunction, membrane lipid peroxidation, protein oxidation, and DNA fragmentation. As the exposure time extends, these damages exceed the cell's repair capacity, ultimately triggering apoptosis (programmed cell death). Notably, the interplay between H_2O_2 and nitrite may generate peroxynitrite, a highly reactive oxidant capable of diffusing into intracellular compartments and causing widespread biochemical injury. Together, these findings highlight that the duration of plasma exposure and the time allowed for cellular interaction with PAW are critical factors in determining its therapeutic potential. The delayed but intensified cytotoxic effect at 48 h reinforces the idea of persistent oxidative stress and supports future exploration of PAW as a time-sensitive anti-cancer treatment strategy [34].

To evaluate the biocompatibility and therapeutic selectivity of plasma-activated water (PAW), we tested its cytotoxicity on normal cells using the MTT

Table 3. RONS concentration and cell viability at different treatment times.

Time (minutes)	H_2O_2 (ppm)	NO_2 (ppm)	NO_3 (ppm)	Viability % 24 h	Viability % 48 h
0	0	0	0	98.10933	98.10933
5	90	10	250	59.375	49.30567
10	100	25	260	51.96767	44.483
15	140	50	300	46.45067	34.95367
20	200	60	450	34.684	25.07733

assay. Our results showed no significant reduction in viability after 5 min of exposure, with cell survival remaining above 95 % at both 24 and 48 h (see Fig. 7). A modest yet statistically significant decline was observed at 10 min ($p < 0.01$), and a more marked reduction at 15 and 20 min ($p < 0.0001$), particularly after 48 h. Nevertheless, all values remained above the 70 % biocompatibility threshold. These findings are consistent with previous reports indicating selective cytotoxicity of PAW in cancer cells due to their higher basal ROS levels and reduced antioxidant defenses [35]. In addition, previous studies have shown that PAW and plasma-activated media selectively impair tumor survival by downregulating pivotal signaling molecules such as the Akt kinase [36,37]. A therapeutic window is supported by the observed low cytotoxicity in normal cells, making PAW a promising candidate for minimal side effects and selective cancer treatment [38].

The analysis revealed a strong reverse relationship between the concentration of (RON) in plasma-active water (PAW) and the viability of MCF-7 cells. High RONS concentrations were associated with a noticeable reduction in cell viability. This supported the hypothesis that the PAW's oxidative content is the most critical driver of its cytotoxic effects, as shown in Fig. 8.

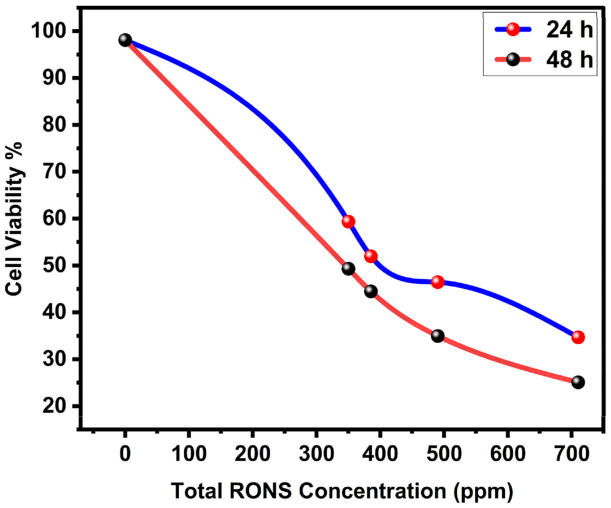

Fig. 8. Relationship between total RONS levels in PAW and MCF-7 cell viability at 24 h and 48 h.

3.6. Mechanism of apoptosis induction

3.6.1. Cell viability reduction (VCC)

Analysis in our experiments revealed a substantial reduction in the number of surviving cells after plasma-activated water (PAW) treatment for 15 and 20 min, as shown in Fig. 9. This decrease suggests cytotoxic effects likely associated with regulated forms of cell death. While the VCC assay alone does not determine the exact mode of death, the observed time-dependent decline in viability supports a non-random, possibly programmed mechanism. Consistent with prior findings, VCC reduction should be interpreted cautiously and complemented with additional molecular assays—such as Total Nuclear Integrity (TNI) and Mitochondrial Membrane Potential (MMP)—to confirm apoptosis as the underlying pathway [39,40].

3.6.2. Total nuclear integrity (TNI)

As illustrated in Fig. 10, the results of the TNI assay revealed a marked increase in intracellular

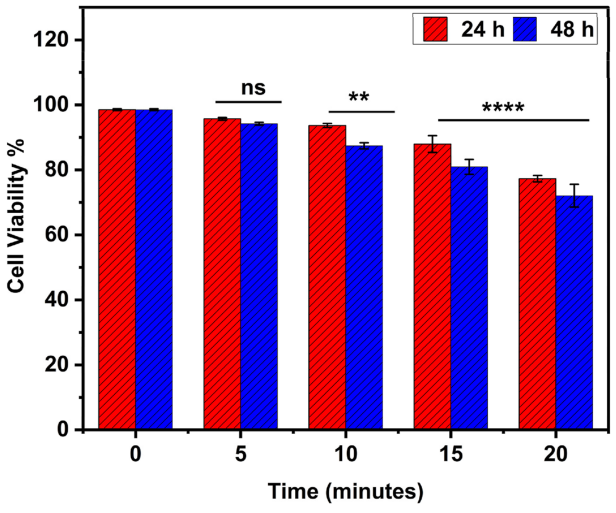

Fig. 7. MTT assay results for MCF-10A after treatment with PAW.

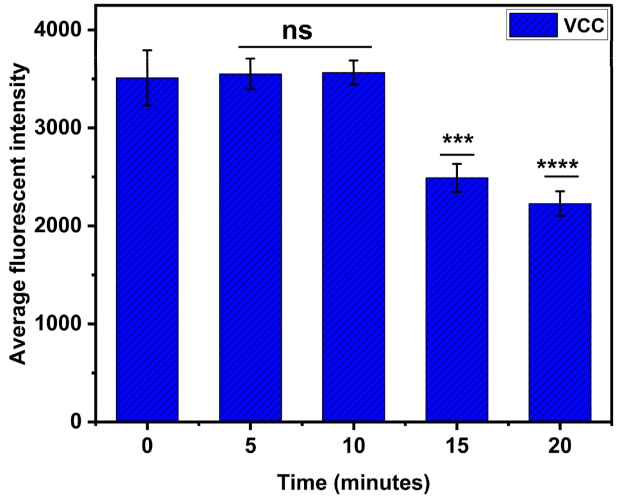

Fig. 9. Time-dependent VCC assay for MCF-7 cells following PAW treatment.

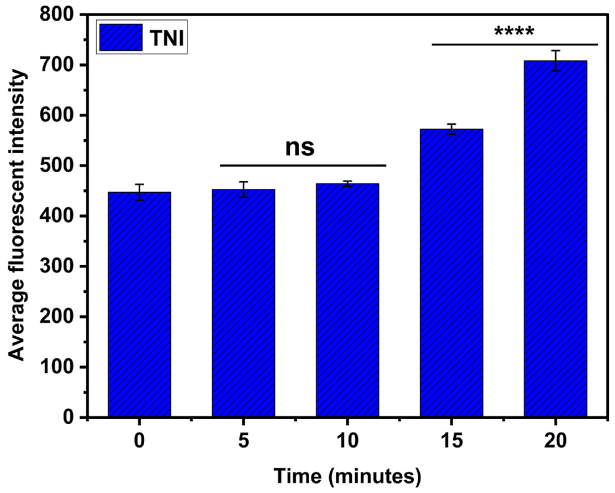

Fig. 10. TNI assay for MCF-7 cells exposed to plasma-activated water.

damage markers following 15 and 20 min of exposure to plasma-activated water. This elevation indicates compromised membrane integrity and potential early-stage apoptosis. The observed rise is likely due to the accumulation of reactive oxygen and nitrogen species (RONS), which induce oxidative stress within the cell. When such damage surpasses the cellular repair threshold, signaling cascades affect organelles such as mitochondria. These outcomes align with prior findings suggesting that RONS-mediated stress can activate intrinsic apoptotic pathways [40].

3.6.3. Mitochondrial dysfunction (MMP)

The mitochondrial membrane potential (MMP) assay, depicted in Fig. 11, confirmed significant dysfunction after 15 and 20 min of treatment with plasma-activated water. A notable decline in MMP was detected—an indicator of mitochondrial collapse and a hallmark of the intrinsic apoptotic pathway. This reduction likely promotes the release of apoptogenic factors such as cytochrome *c* into the cytoplasm, contributing to programmed cell death. Our results are consistent with previous findings [41], suggesting that plasma-activated water may induce apoptosis via mitochondrial-mediated mechanisms.

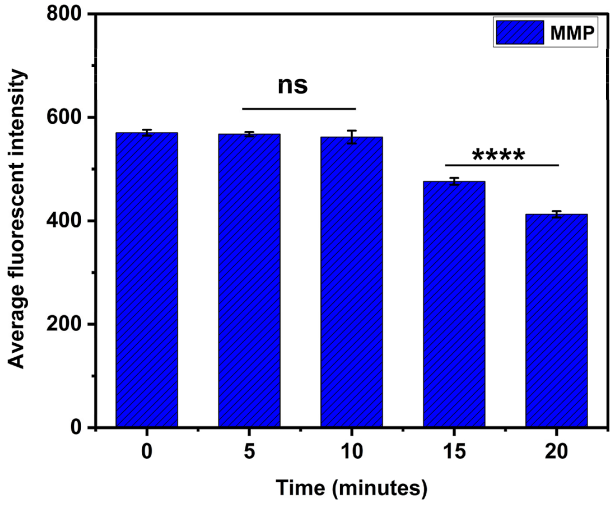

Fig. 11. Assessment of mitochondrial membrane potential (MMP) following PAW treatment.

4. Conclusion

In conclusion, this study demonstrated the therapeutic potential of plasma-activated water (PAW) generated using a novel dielectric barrier discharge (DBD) plasma system equipped with a micromesh electrode and a nitrogen–argon gas mixture. The improved plasma configuration significantly enhanced the physicochemical properties of the treated water, primarily through the elevation of reactive oxygen and nitrogen species (RONS), which were associated with increased cytotoxicity toward breast cancer cells. An apparent time-dependent effect was observed, with significantly higher levels of cell death after 48 h compared to 24 h. Cellular assays revealed that PAW induced programmed cell death through multiple mechanisms, including mitochondrial dysfunction, nuclear alterations, and reduced cell viability, as indicated by changes in mitochondrial membrane potential (MMP), viable cell count (VCC), and Total Nuclear Integrity (TNI). These findings suggest that PAW disrupts essential bioenergetic and structural processes, activating cell death pathways. Preliminary evaluation on normal cells showed promising results, indicating lower cytotoxicity compared to cancer cells and supporting the potential selective action of PAW. More complex biological models may offer deeper insights into their therapeutic behavior in dynamic cellular environments. These models include three-dimensional (3D) tumor cultures and co-culture systems replicating the tumor microenvironment, providing a more accurate representation of biological responses and biosafety under conditions that closely resemble clinical applications. Furthermore, combining PAW with other therapeutic strategies—such as chemotherapy, radiotherapy, or nanoparticle-based drug delivery—may enhance its anticancer efficacy while reducing systemic toxicity. Understanding PAW's large-scale production, storage stability, and clinical implementation mechanisms is essential for translating these findings into practical biomedical solutions.

Ethics approval

This study used commercially available cell lines and did not involve human or animal subjects. Therefore, ethical approval and informed consent were not required.

Funding

This research received no external funding.

Conflicts of interest

The authors declare that they have no competing interests.

Acknowledgments

The authors would like to thank the Department of Physics, College of Science, University of Baghdad, for the support provided during the research. The Iraqi Ministry of Higher Education and Scientific Research also supported this work.

References

[1] Q. Wang, D. Salvi, Recent progress in the application of plasma-activated water (PAW) for food decontamination, Curr. Opin. Food Sci. 42 (2021) 51–60, https://doi.org/10.1016/j.cofs.2021.04.012.

[2] X. Chen, Y. Cheng, T. Li, Y. Cheng, Characteristics and applications of plasma-assisted chemical processes and reactors, Curr. Opin. Chem. Eng. 17 (2017) 68–77, https://doi.org/10.1016/J.COCHE.2017.07.001.

[3] L. Boeckmann, M. Schäfer, T. Bernhardt, M.L. Semmler, O. Jung, G. Ojak, T. Fischer, K. Peters, B. Nebe, B. Müller-Hilke, C. Seebauer, S. Bekeschus, S. Emmert, Cold atmospheric pressure plasma in wound healing and cancer treatment, Appl. Sci. 10 (2020) 6898, https://doi.org/10.3390/app10196898.

[4] N.K. Kaushik, B. Ghimire, Y. Li, M. Adhikari, M. Veerana, N. Kaushik, N. Jha, B. Adhikari, S.-J. Lee, K. Masur, T. Von Woedtke, K.-D. Weltmann, E.H. Choi, Biological and medical applications of plasma-activated media, water and solutions, Biol. Chem. 400 (2018) 39–62, https://doi.org/10.1515/hsz-2018-0226.

[5] B. Pang, Z. Liu, Y. Gao, X. Li, S. Wang, Q. Miao, X. Zhao, R. Fan, D. Xu, P.J. Cullen, R. Zhou, Enhanced anticancer efficacy of alkaline plasma-activated water through augmented RONS production, ACS Appl. Mater. Interfaces 17 (2024) 467–483, https://doi.org/10.1021/acsami.4c16518.

[6] P.R. Rotondo, D. Aceto, M. Ambrico, A.M. Stellacci, F. Faretra, R.M. De Miccolis Angelini, P.F. Ambrico, Physicochemical properties of plasma-activated water and associated antimicrobial activity against fungi and bacteria, Sci. Rep. 15 (2025) 5536, https://doi.org/10.1038/s41598-025-88369-7.

[7] S. Mohades, A.M. Lietz, M.J. Kushner, Generation of reactive species in water film dielectric barrier discharges sustained in argon, helium, air, oxygen, and nitrogen, J. Phys. D Appl. Phys. 53 (2020) 435206, https://doi.org/10.1088/1361-6463/aba21a.

[8] B. Pang, Z. Liu, S. Wang, Y. Gao, M. Qi, D. Xu, R. Zhou, D. Liu, M.G. Kong, Alkaline plasma-activated water (PAW) as an innovative therapeutic avenue for cancer treatment, Appl. Phys. Lett. 121 (2022) 144101, https://doi.org/10.1063/5.0107906.

[9] E. Griseti, N. Merbahi, M. Golzio, Anti-cancer potential of two plasma-activated liquids: implication of long-lived reactive oxygen and nitrogen species, Cancers 12 (2020) 721, https://doi.org/10.3390/cancers12030721.

[10] J. Zhang, T. Wu, Z. Wang, S. Xu, X. Jing, Z. Zhang, J. Lin, H. Zhang, D. Liu, R. Zhou, L. Guo, X. Wang, M. Rong, Y. Shao, K.K. Ostrikov, Plasma-generated RONS in liquid transferred into cryo-microneedles patch for skin treatment of melanoma, Redox Biol. 75 (2024) 103284, https://doi.org/10.1016/j.redox.2024.103284.

[11] F. Girard, M. Peret, N. Dumont, V. Badets, S. Blanc, K. Gazeli, C. Noël, T. Belmonte, L. Marlin, J.-P. Cambus, G. Simon, N. Sojic, B. Held, S. Arbault, F. Clément, Correlations between gaseous and liquid phase chemistries induced by cold atmospheric plasmas in a physiological buffer, Phys. Chem. Chem. Phys. 20 (2018) 9198–9210, https://doi.org/10.1039/C8CP00264A.

[12] G.G. Bălan, I. Roşca, E.-L. Ursu, F. Doroftei, A.-C. Bostănaru, E. Hnatiuc, V. Năstasă, V. Șandru, G. Ștefănescu, A. Trifan, M. Mareş, Plasma-activated water: a new and effective alternative for duodenoscope reprocessing, Infect. Drug Resist. 11 (2018) 727–733, https://doi.org/10.2147/IDR.S159243.

[13] S. Zahedian, A. Hekmat, S.H. Tackallou, M. Ghoranneviss, The impacts of prepared plasma-activated medium (PAM) combined with doxorubicin on the viability of MCF 7 breast cancer cells: a new cancer treatment strategy, Rep. Biochem. Mol. Biol. 10 (2022) 640–652, https://doi.org/10.52547/rbmb.10.4.640.

[14] S. Raud, J. Raud, I. Jõgi, C.-T. Piller, T. Plank, R. Talviste, T. Teesalu, E. Vasar, The production of plasma activated water in controlled ambient gases and its impact on cancer cell viability, Plasma Chem. Plasma Process. 41 (2021) 1381–1395, https://doi.org/10.1007/S11090-021-10183-6.

[15] M. Ghasemi, T. Turnbull, S. Sebastian, I. Kempson, The MTT assay: utility, limitations, pitfalls, and interpretation in bulk and single-cell analysis, Int. J. Mol. Sci. 22 (2021) 12827, https://doi.org/10.3390/ijms222312827.

[16] D. Durán Martínez, A. Valladares Méndez, J. Rivera Islas, J. N. Sánchez Carranza, Studies of applications of cold plasma systems in cancer treatment: mechanisms of oxidant stress and pathway signaling, Stresses 4 (2024) 896–915, https://doi.org/10.3390/stresses4040060.

[17] V.V. Kovačević, B. Dojčinović, M. Jović, G. Roglić, B.M. Obradović, M.M. Kuraica, Measurement of reactive species generated by dielectric barrier discharge in direct contact with water in different atmospheres, J. Phys. D Appl. Phys. 50 (2017) 155205, https://doi.org/10.1088/1361-6463/aa5fde.

[18] A. Kumar, V.K. Sai, Y. Huaccallo-Aguilar, S.F. Reinecke, U. Hampel, Characterization of reactive species in water induced by cold atmospheric air plasma: experimental applications for industrial micropollutant removal from wastewater and seed germination, J. Environ. Chem. Eng. 13 (2025) 117263, https://doi.org/10.1016/j.jece.2025.117263.

[19] B.R. Locke, S.M. Thagard, Analysis and review of chemical reactions and transport processes in pulsed electrical discharge plasma formed directly in liquid water, Plasma Chem. Plasma Process. 32 (2012) 875–917, https://doi.org/10.1007/s11090-012-9403-y.

[20] W. Van Gaens, A. Bogaerts, Kinetic modelling for an atmospheric pressure argon plasma jet in humid air, J. Phys. D: Appl. Phys. 46 (2013) 275201, https://doi.org/10.1088/0022-3727/46/27/275201.

[21] D. Terefinko, A. Dzimitrowicz, A. Bielawska-Pohl, P. Jamroz, The influence of cold atmospheric pressure plasma-treated media on the cell viability, motility, and induction of apoptosis in human non-metastatic (MCF7) and metastatic (MDA-MB-231) breast cancer cells, Int. J. Mol. Sci. 22 (2021) 3855, https://doi.org/10.3390/ijms22083855.

[22] J. Debnath, S.K. Muthuswamy, J.S. Brugge, Morphogenesis and oncogenesis of MCF-10A mammary epithelial cells,

Methods 30 (2003) 256–268, https://doi.org/10.1016/S1046-2023(03)00032-X.
[23] J. Van Meerloo, G.J.L. Kaspers, J. Cloos, Cell sensitivity assays: the MTT assay, Methods Mol. Biol. 731 (2011) 237–245, https://doi.org/10.1007/978-1-61779-080-5_20.
[24] A. Qayyum, S. Zeb, M.A. Naveed, N.U. Rehman, S.A. Ghauri, M. Zakaullah, Optical emission spectroscopy of Ar–N_2 mixture plasma, J. Quant. Spectrosc. Ra. 107 (2007) 361–371, https://doi.org/10.1016/j.jqsrt.2007.02.008.
[25] M.G. Jasim, Q.A. Abbas, Influence of the homogeneous magnetic field on the laser-induced breakdown spectroscopy of copper plasma, Iraqi J. Sci. 59 (2018) 2217–2224. https://ijs.uobaghdad.edu.iq/index.php/eijs/article/view/550.
[26] M.G. Jasim, Q.A. Abbas, Influence of working pressure and lasing energy of Al plasma in laser-induced breakdown spectroscopy, Iraqi J. Phys. 17 (2019) 59–66, https://doi.org/10.30723/ijp.v17i40.406.
[27] A. Qusnudin, K. Kusumandari, T.E. Saraswati, OH Radical Intensity of dielectric barrier discharge (DBD) plasma measured by optical emission spectroscopy (OES), J. Phys. Conf. Ser. 1825 (2021) 012072, https://doi.org/10.1088/1742-6596/1825/1/012072.
[28] R. Thirumdas, A. Kothakota, U.S. Annapure, K. Siliveru, R. Blundell, R. Gatt, V.P. Valdramidis, Plasma activated water (PAW): chemistry, physicochemical properties, applications in food and agriculture, Trends Food Sci. Tech. 77 (2018) 21–31, https://doi.org/10.1016/j.tifs.2018.05.007.
[29] H. Jablonowski, T. von Woedtke, Research on plasma medicine-relevant plasma–liquid interaction: what happened in the past five years? Clin. Plasma Med. 3 (2015) 42–52, https://doi.org/10.1016/j.cpme.2015.11.003.
[30] F.A. Naeim, H.R. Humud, The effect of gas flow rate, exposure times, and ageing on the physicochemical properties of water activated by glow discharge plasma jet, E. Eur. J. Phys. 2 (2023) 370–377, https://doi.org/10.26565/2312-4334-2023-2-43.
[31] K. Kučerová, M. Henselová, Ľ. Slováková, M. Bačovčinová, K. Hensel, Effect of plasma activated water, hydrogen peroxide, and nitrates on lettuce growth and its physiological parameters, Appl. Sci. 11 (2021) 1985, https://doi.org/10.3390/app11051985.
[32] F.A. Naeim, H.R. Humud, Studying the physicochemical properties of water activated by microwave-induced plasma jet for biological and medical applications, Acta Phys. Pol. A. 144 (2023) 81–86, https://doi.org/10.12693/APhysPolA.144.81.
[33] J.H. Bae, H. Lee, S.-C. Huh, S. Park, Nitric and nitrous acid formation in plasma-treated water: decisive role of nitrogen oxides (NO=1–3), Chemosphere 364 (2024) 143105, https://doi.org/10.1016/j.chemosphere.2024.143105.
[34] D. Terefinko, A. Dzimitrowicz, A. Bielawska-Pohl, A. Klimczak, P. Pohl, P. Jamroz, The influence of cold atmospheric pressure plasma-treated media on the cell viability, motility, and induction of apoptosis in human Non-Metastatic (MCF7) and metastatic (MDA-MB-231) breast cancer cell lines, Int. J. Mol. Sci. 22 (2021) 3855, https://doi.org/10.3390/ijms22083855.
[35] D. Yan, J.H. Sherman, M. Keidar, Cold atmospheric plasma, a novel promising anti-cancer treatment modality, Oncotarget 8 (2017) 15977–15995, https://doi.org/10.18632/oncotarget.13304.
[36] H. Tanaka, M. Mizuno, K. Ishikawa, K. Nakamura, H. Kajiyama, H. Kano, F. Kikkawa, M. Hori, Plasma-activated medium selectively kills glioblastoma brain tumor cells by down-regulating a survival signaling molecule, AKT kinase, Plasma Med. 1 (2011) 265–277, https://doi.org/10.1615/PlasmaMed.2012006275.
[37] A.P. Subramanian, V.P. Veeraraghavan, C. Senthilkumar, Y. L. Yeh, W.W. Kuo, P. Geraldine, Plasma-activated water from a dielectric barrier discharge plasma source for the selective treatment of cancer cells, Plasma Process. Polym. 17 (2020) 1900260, https://doi.org/10.1002/ppap.201900260.
[38] G. Fridman, G. Friedman, A. Gutsol, A.B. Shekhter, V.N. Vasilets, A. Fridman, Applied plasma medicine, Plasma Process. Polym. 5 (2008) 503–533, https://doi.org/10.1002/ppap.200700154.
[39] W. Strober, Trypan blue exclusion test of cell viability, Curr. Protoc. Immunol. 21 (2001) A.3B.1–A.3B.2, https://doi.org/10.1002/0471142735.ima03bs21.
[40] T. Adachi, H. Tanaka, S. Nonomura, H. Hara, S. Kondo, M. Hori, Plasma-activated medium induces A549 cell injury via a spiral apoptotic cascade involving the mitochondrial-nuclear network, Free Radic. Biol. Med. 79 (2015) 28–44, https://doi.org/10.1016/J.FREERADBIOMED.2014.11.014.
[41] G. Kroemer, J.C. Reed, Mitochondrial control of cell death, Nat. Med. 6 (2000) 513–519, https://doi.org/10.1038/74994.